

Substructuring of the Dynamic Substructures Round Robin Test Bed



Authors:

Daniel Roettgen

Garrett Lopp

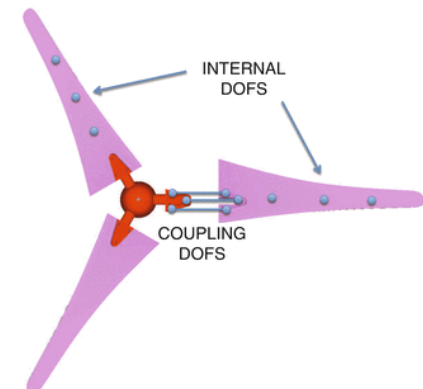
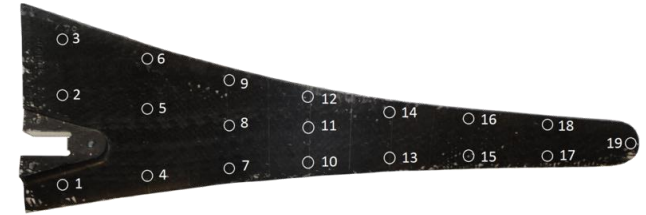
Ben Moldenhauer

Anthony Jaramillo

Special Guest Speaker: Andreas Linderholt

Background

- The substructuring community has a rich history which shares its roots with model reduction and structural modification
- Each year we see 4-5 sessions on substructuring at IMAC with various topics including:
 - Component Mode Synthesis
 - Frequency Based Substructuring
 - Transfer Path Analysis
 - Model Reduction
 - Applications of Substructuring
 - Real-time Hybrid Substructuring and many more
- In 2012 the AmpAir 600 Wind Turbine was selected as a round-robin substructuring example that many universities and research groups have studied
- The Dynamic Substructuring focus group continued organizing IMAC sessions and in 2018 it officially became a technical division.

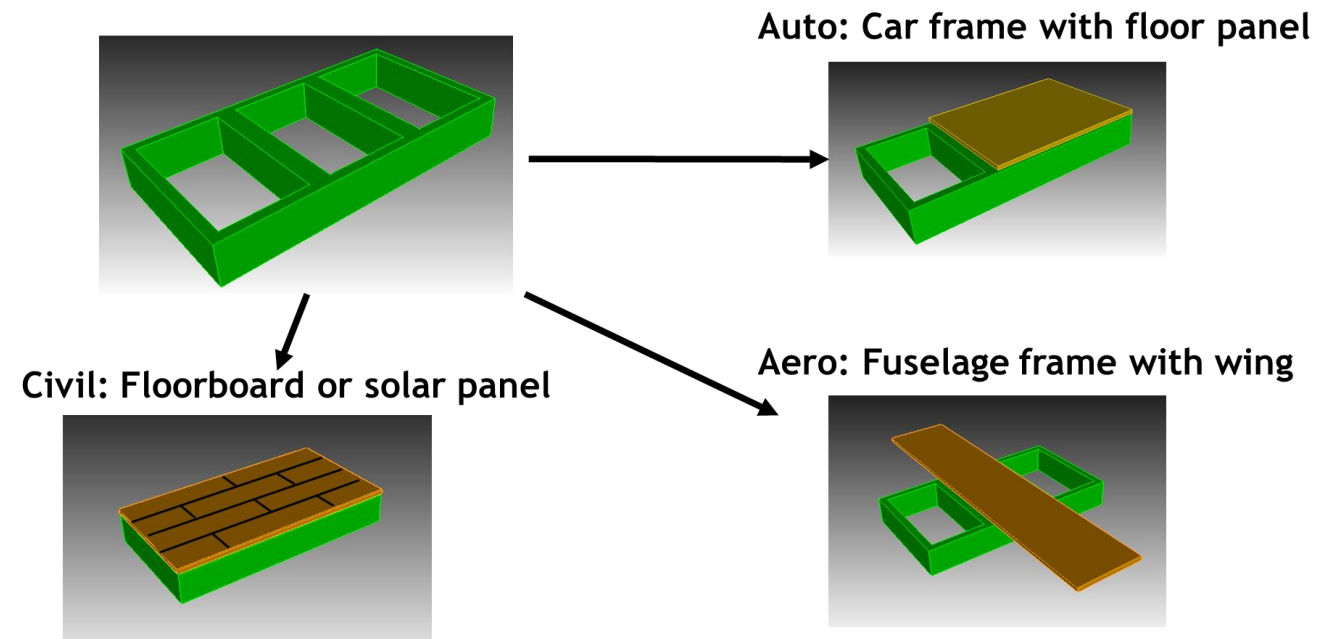
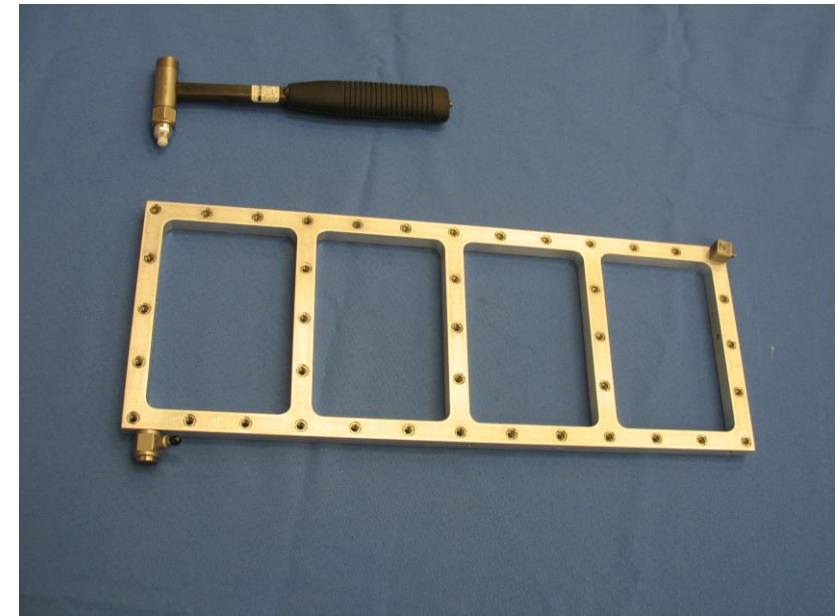


Experimental Substructure (Four-unit frame)

- Team developed design for a “four-unit” frame

Key features

- Manufactured from one piece of metal of stock
- Subcomponent and shaker attachment points machined into frame
- Adaptable to many types of studies
- Possible circular/recursive transfer path
- Large enough to minimize error due to mass loading

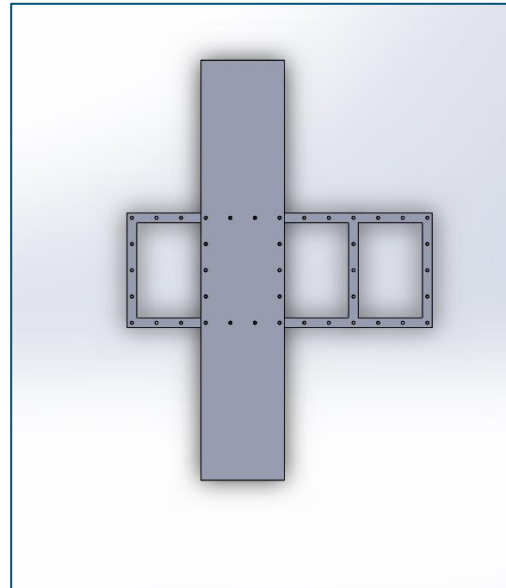


Shown is a 3-unit frame (final design has 4 units)

Substructuring Round-Robin Procedure



- Participants will be provided:
 - Hardware of the frame, rectangular thin wing, rectangular thick wings, and necessary fasteners
 - Assembly Procedure
 - Solid Models of the Rectangular Wings
 - **Models and test data soon to be available on the substructuring wiki!**
- Researchers can demonstrate their substructuring techniques using the rectangular wing hardware then predict the change from a thin to thick wing
- System can be tested with connection at just corner holes, or all 14 holes



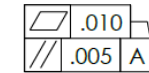
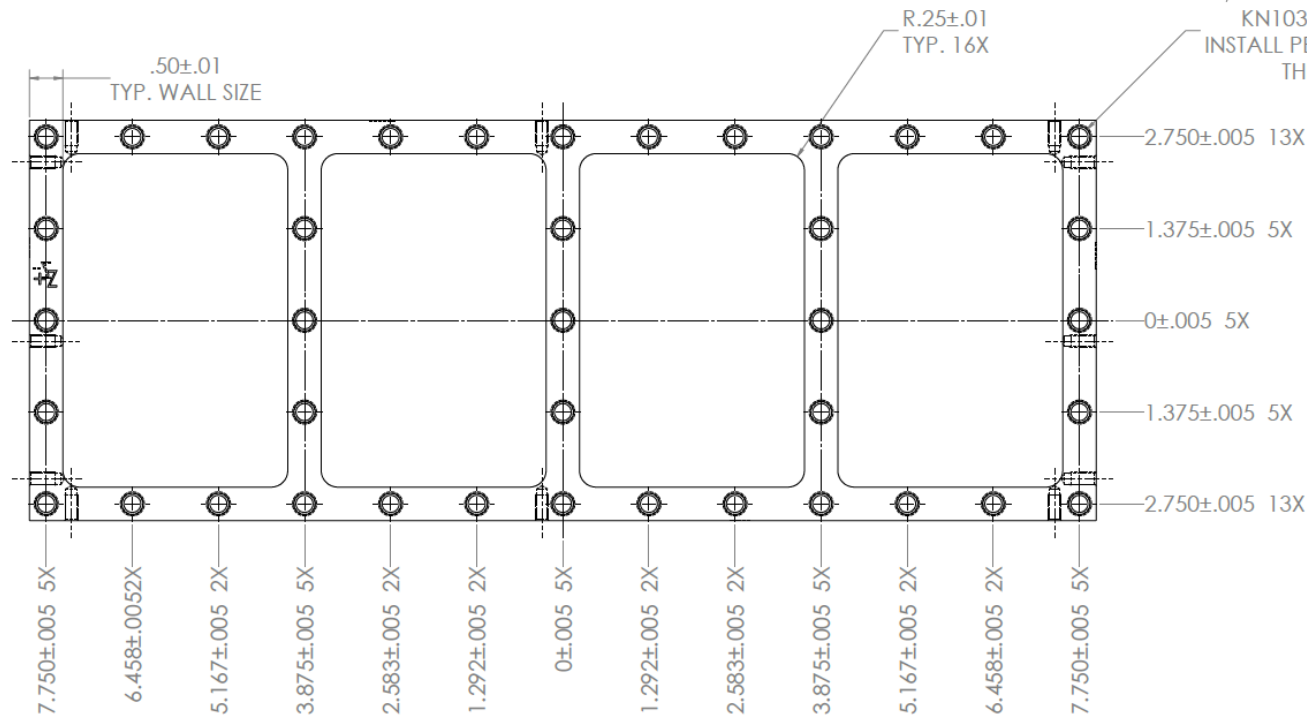
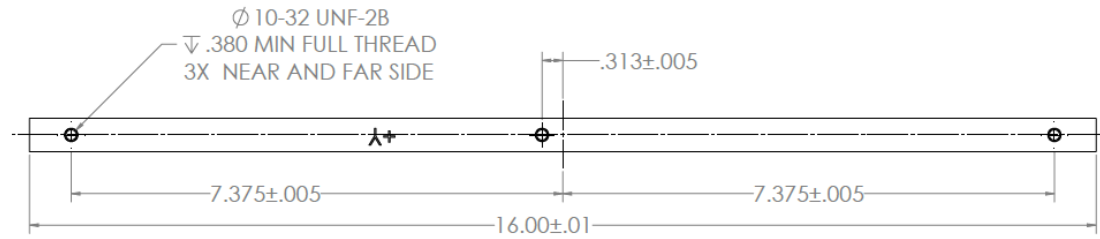
What is the “truth” answer?

- Truth depends on a lot of factors:
 - Assembly procedure
 - Frequency range of interest
 - Linearity of joints
 - And other factors...
- The goal of this round-robin isn't to see which method is the closest to truth
- Instead... Round-Robin goals include:
 - Fostering collaboration between universities and industrial researchers
 - Helping researchers focus on how to best approach a substructuring problem when truth is unknown
 - Discuss different approaches taken and why some methods are more suited for specific connection interfaces
 - See range of blind predictions to understand the range of answer found using substructuring practices

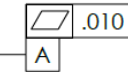


It depends... but we can learn a lot by comparing and collaborating on methods

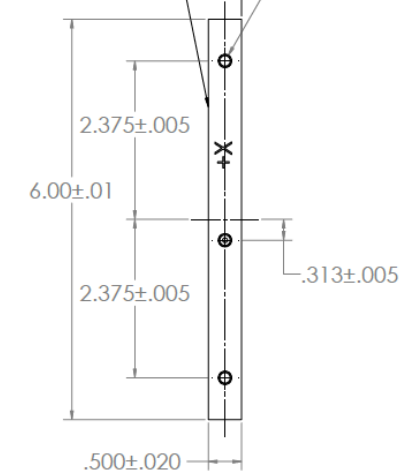
Frame Details



ϕ DRILL AND TAP FOR KN1032 KEENSERT
INSTALL PER MFG. SPECS THRU 41X



$\phi 10-32 \text{ UNF-2B}$
 $\nabla .380 \text{ MIN FULL THREAD}$
3X NEAR AND FAR SIDE



NOTES:

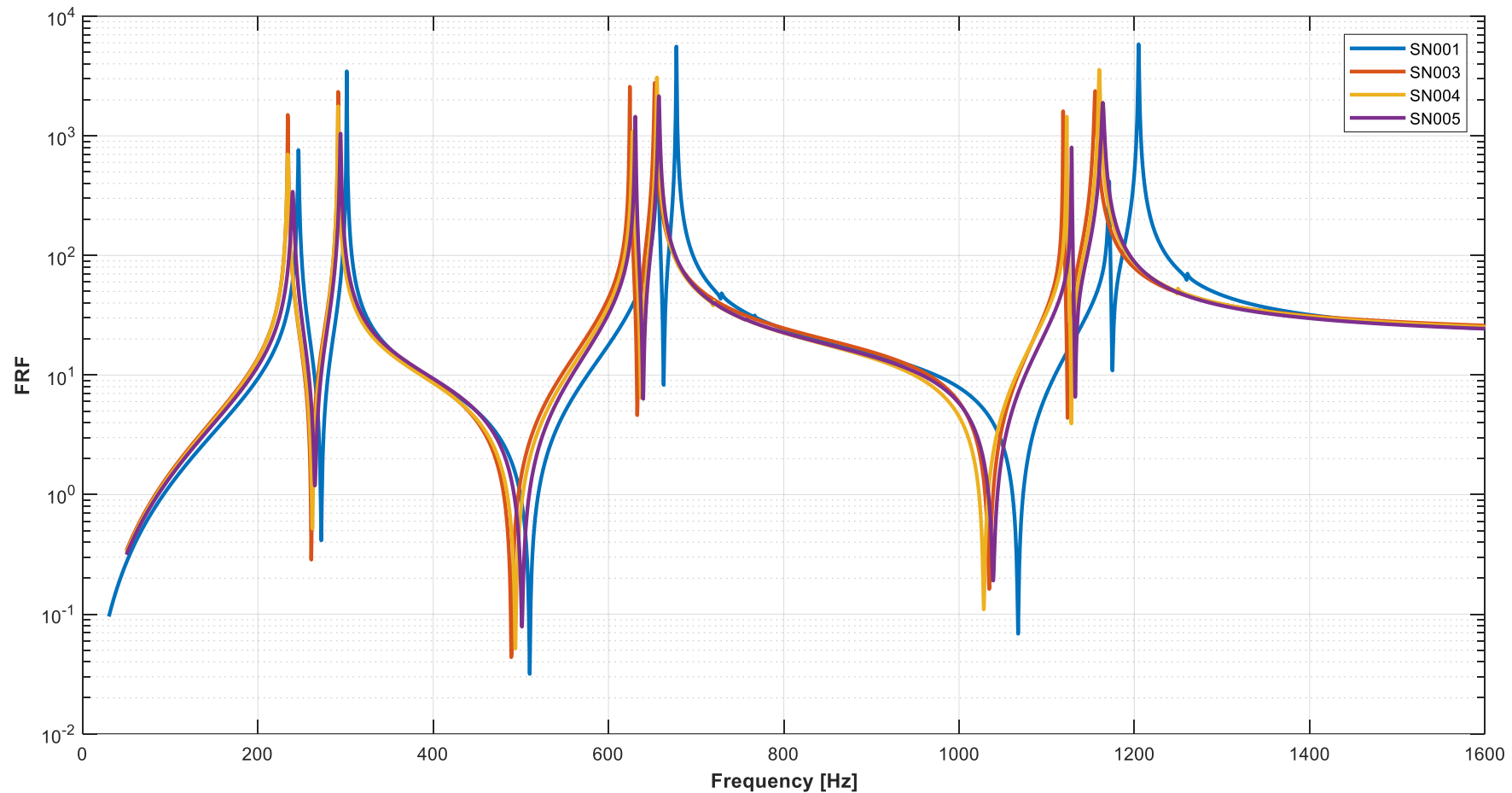
1. ALL WORK PER 9900000
2. MATERIAL- ALUMINUM
TYPE: 6061-T6
3. 1 REQUIRED

FOUR UNIT FRAME,
SSBB

D 111319MODDRSS10-01 1 1

Frame Measurements

- 5 frames available
- 5 more in production

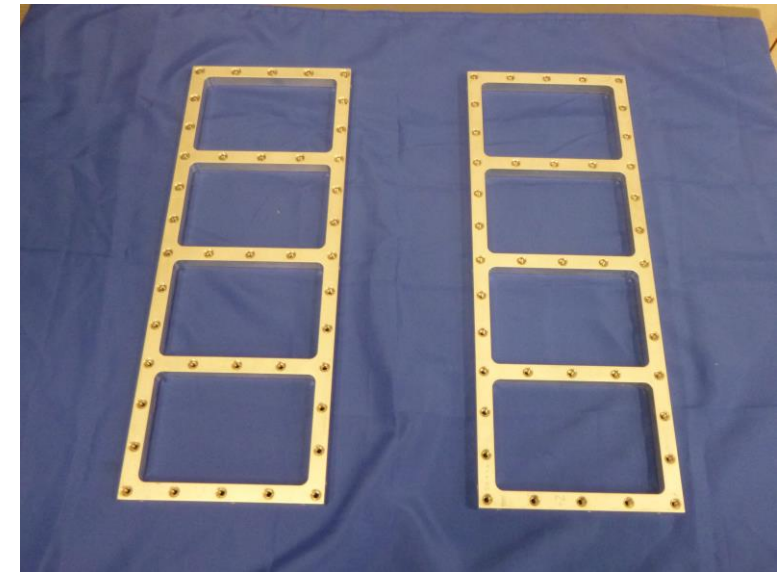


5 Frames manufactured and measured – data soon to be available on the TD wiki!

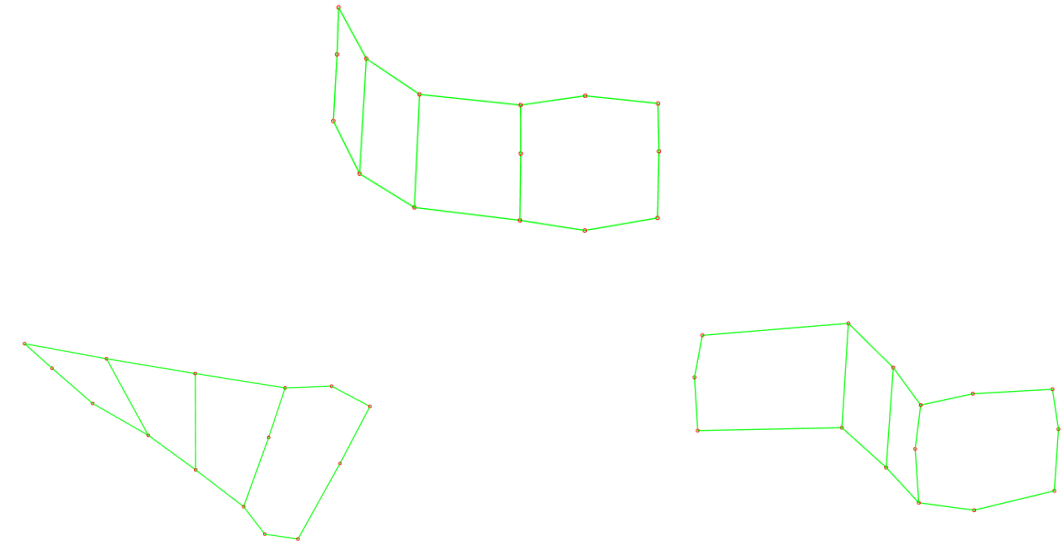
Frame Data Available

- Weights by serial number
- Mode Shapes by serial number
- Geometry to modes by serial number
- Mode shape gifs
- Solid model

Frame	Weight [lb]
SN001	1.381
SN002	1.376
SN003	1.379
SN004	1.372
SN005	1.371



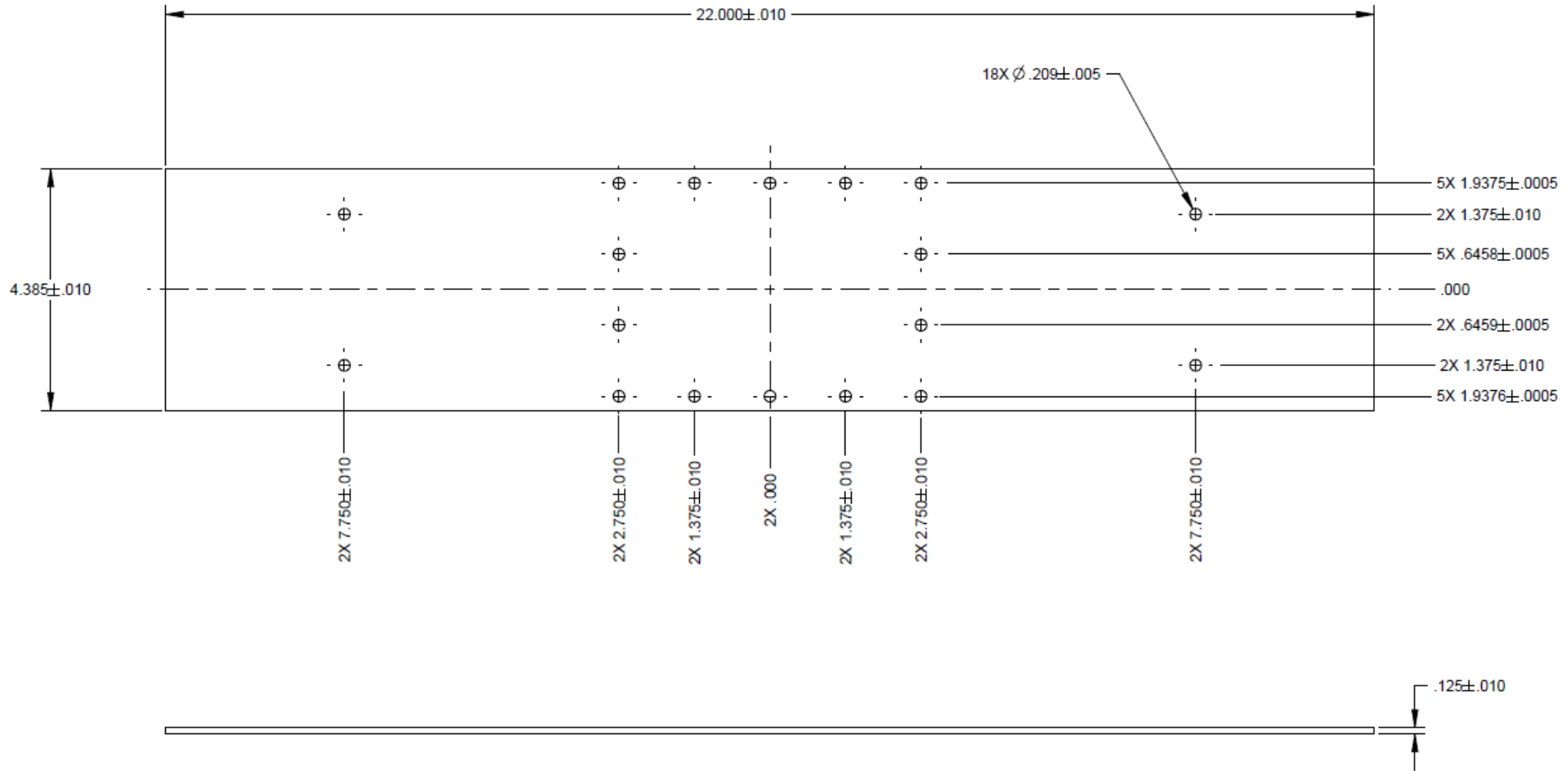
	Frequencies					
Mode	SN001	SN002	SN003	SN004	SN005	Mean
1	246.25	237.81	234.18	234.18	239.69	238.42
2	301.41	294.52	291.71	291.42	294.23	294.66
3	656.09	632.50	624.38	627.50	630.63	634.22
4	677.50	659.38	652.81	655.31	657.50	660.50
5	728.59	719.69	715.31	719.69	720.31	720.72
6	766.65	755.63	751.99	754.06	756.56	756.98
7	1171.25	1132.81	1118.75	1122.81	1128.50	1134.82
8	1204.84	1167.81	1155.31	1160.00	1164.06	1170.41
9	1260.16	1247.19	1241.27	1249.38	1249.38	1249.47



Data soon to be available on the TD wiki!

Wing Details

- 1/8th and 1/4th inch thick wings exist

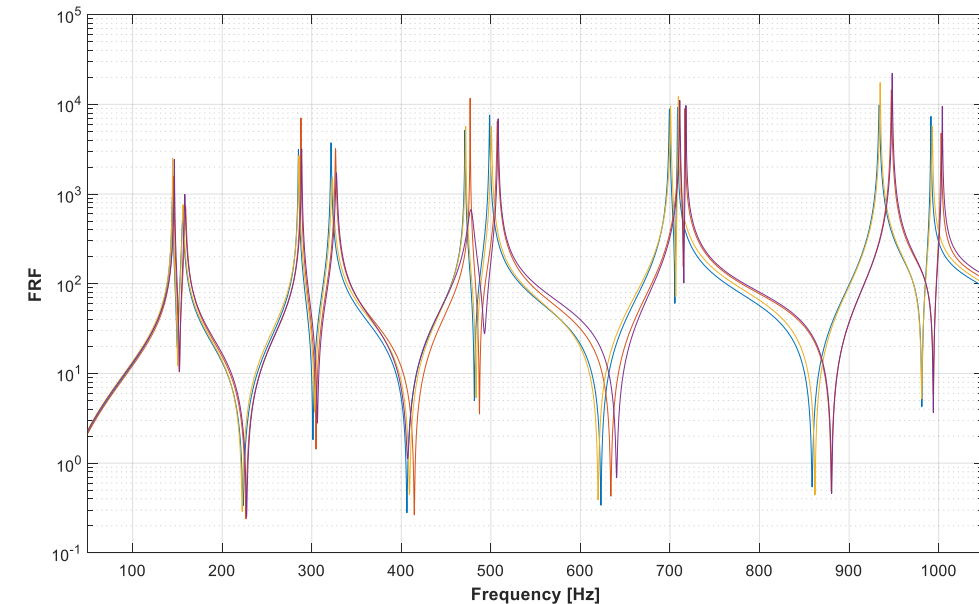
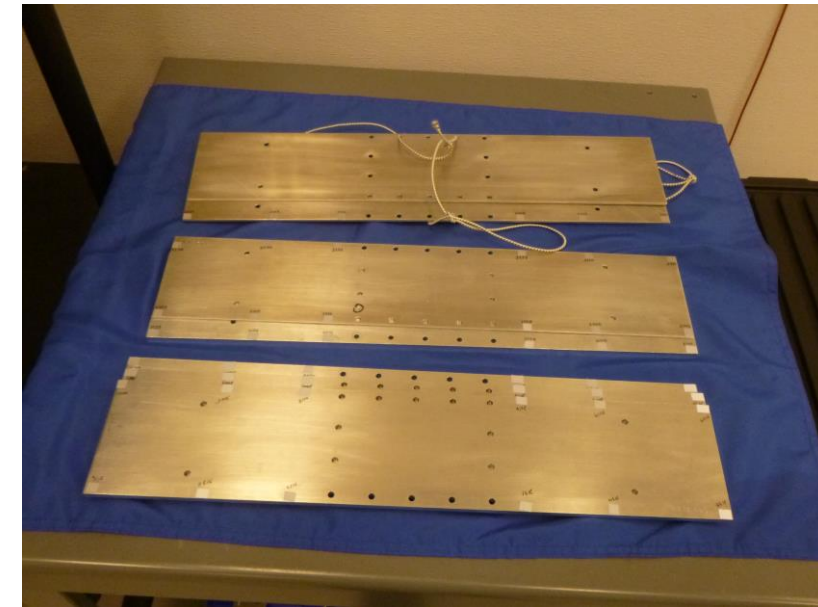


Wing Measurements

- 5 wing pairs available, 5 more in production

Thin Wing	Weight [lb]	Thick Wing	Weight [lb]
Wing001A	1.545	Wing001B	2.4905
Wing002A	1.1615	Wing002B	2.48
Wing003A	1.152	Wing003B	2.498
Wing004A	1.6145	Wing004B	2.4975
Wing005A	1.1615	Wing005B	2.4945

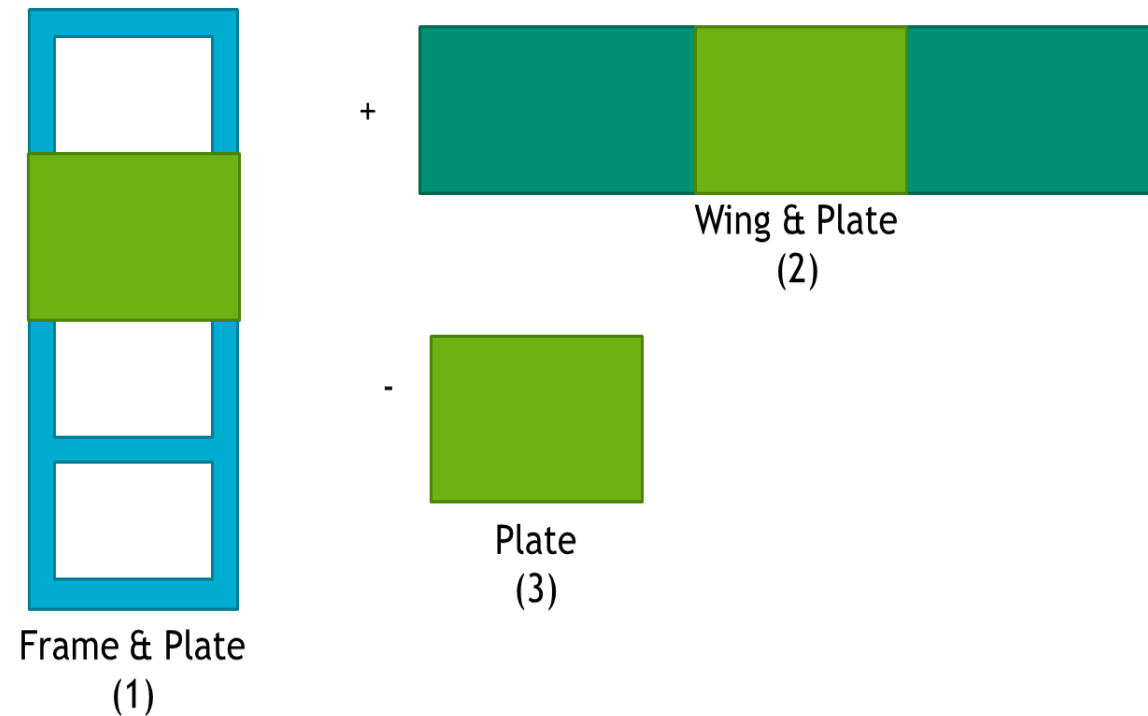
	Frequencies					
Mode	SN001	SN002	SN003	SN004	SN005	Mean
1	144.45	146.01	144.69	146.56	145.48	145.44
2	155.83	159.00	156.25	158.28	156.87	157.25
3	285.16	287.97	285.77	288.75	287.19	286.97
4	321.56	326.56	322.96	327.50	325.79	324.88
5	471.09	476.88	471.87	477.81	475.00	474.53
6	498.59	507.19	500.56	508.13	505.31	503.96
7	699.38	710.31	700.63	710.94	707.19	705.69
8	708.40	716.72	709.33	717.81	713.75	713.20
9	933.59	947.19	934.69	948.13	942.81	941.28
10	991.35	1002.78	992.81	1004.06	998.13	997.83



More wing data available soon on the TD wiki!

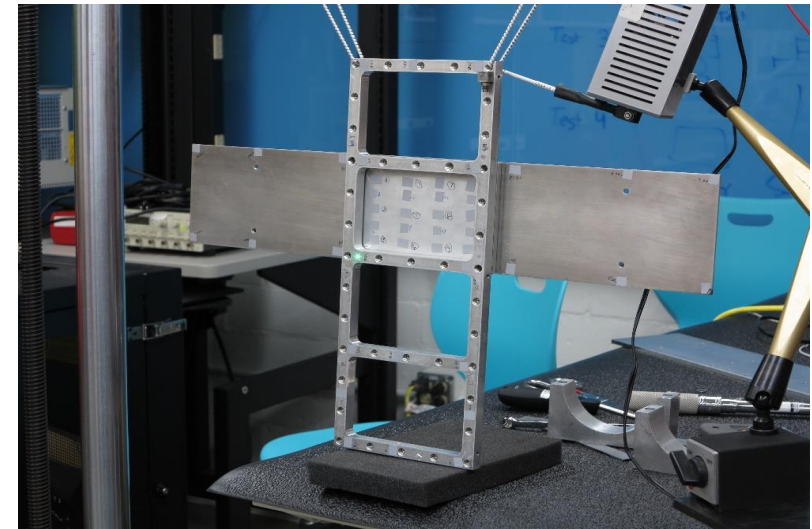
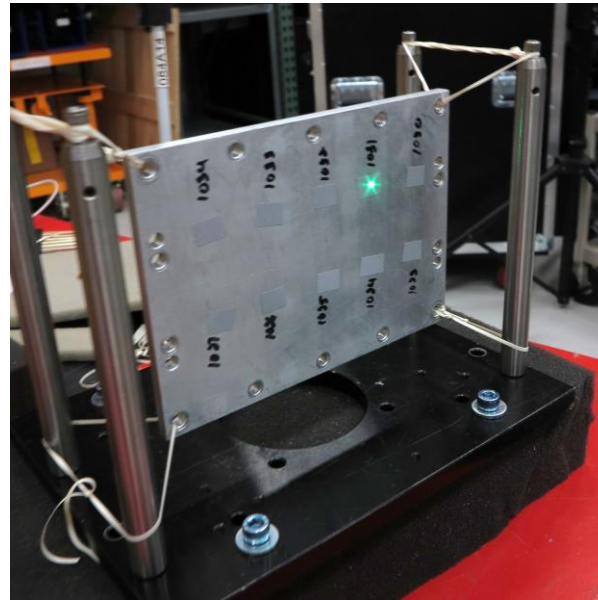
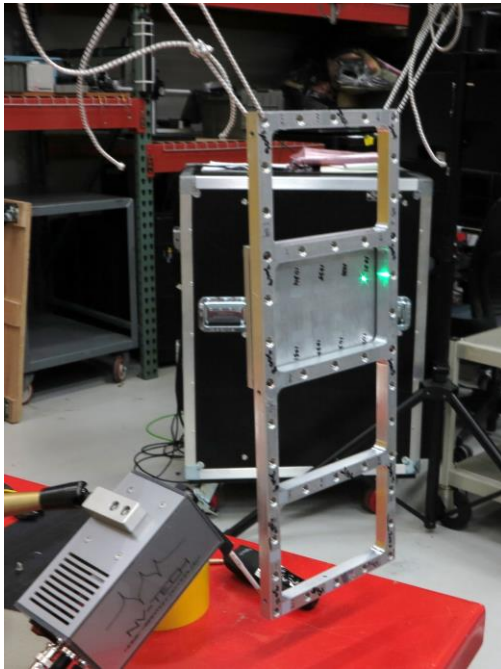
Trial Run

- In the last year SNL performed an updated trial run on the system connecting a frame and wing through a transmission simulator – the goal was to predict system level response



Experiments

- Testing was performed on all three substructures using an LDV (data from these tests will be available on the dynamic substructuring wiki!)



- A truth test was also completed to compare prediction results

Substructuring Mathematics

- To complete substructuring three experimental sets of data were used to fit modal modes for each substructure^{1,2}

$$\begin{bmatrix} I_1 & 0 & 0 \\ 0 & I_2 & 0 \\ 0 & 0 & -I_3 \end{bmatrix} \begin{Bmatrix} \ddot{q}_1 \\ \ddot{q}_2 \\ \ddot{q}_3 \end{Bmatrix} + \begin{bmatrix} [\ddot{\omega}_1^2] & 0 & 0 \\ 0 & [\ddot{\omega}_2^2] & 0 \\ 0 & 0 & -[\ddot{\omega}_3^2] \end{bmatrix} \begin{Bmatrix} q_1 \\ q_2 \\ q_3 \end{Bmatrix} = \begin{Bmatrix} \phi_1^T F_1 \\ \phi_2^T F_2 \\ \phi_3^T F_3 \end{Bmatrix}$$

- Constraints were defined connecting the wing/plate substructure to a lone plate and the frame/plate substructure the same.

$$\begin{bmatrix} \phi_3^+ & 0 \\ 0 & \phi_3^+ \end{bmatrix} \begin{bmatrix} \phi_1 & 0 & -\phi_3 \\ 0 & \phi_2 & -\phi_3 \end{bmatrix} \begin{Bmatrix} q_A \\ q_B \\ q_{TS} \end{Bmatrix} = \tilde{B} \begin{Bmatrix} q_1 \\ q_2 \\ q_3 \end{Bmatrix} = 0$$

- The null space function was used to determine our synthetization matrix L

$$L = \text{null}(\tilde{B})$$

- L-matrix used to enforce constraints on equations of motion and predict system assembly response

$$L^T \begin{bmatrix} I_1 & 0 & 0 \\ 0 & I_2 & 0 \\ 0 & 0 & -I_3 \end{bmatrix} L \begin{Bmatrix} \ddot{q}_1 \\ \ddot{q}_2 \\ \ddot{q}_3 \end{Bmatrix} + L^T \begin{bmatrix} [\ddot{\omega}_1^2] & 0 & 0 \\ 0 & [\ddot{\omega}_2^2] & 0 \\ 0 & 0 & -[\ddot{\omega}_3^2] \end{bmatrix} L \begin{Bmatrix} q_1 \\ q_2 \\ q_3 \end{Bmatrix} = L^T \begin{Bmatrix} \phi_1^T F_1 \\ \phi_2^T F_2 \\ \phi_3^T F_3 \end{Bmatrix}$$

Trial Results

- Predictions led to low frequency and damping error outside of a few modes

Truth		Prediction		Error	
fn	zt	fn	zt	fn	zt
61.91	0.231%	55.76	0.033%	-9.93%	-85.83%
107.19	0.185%	96.16	0.123%	-10.29%	-33.70%
230.00	0.073%	225.92	0.069%	-1.77%	-5.42%
277.66	0.143%	272.85	0.045%	-1.73%	-68.61%
341.56	0.246%	330.92	0.104%	-3.12%	-57.59%
369.06	0.131%	352.90	0.072%	-4.38%	-45.50%
418.91	0.145%	396.28	0.067%	-5.40%	-53.61%
499.06	0.251%	598.74	0.100%	19.97%	-59.96%
656.09	0.103%	611.07	0.116%	-6.86%	12.57%
696.41	0.095%	688.10	0.164%	-1.19%	72.45%
798.75	0.029%	726.60	0.093%	-9.03%	215.58%
807.50	0.084%	733.88	0.069%	-9.12%	-17.92%
857.19	0.197%	784.65	0.119%	-8.46%	-39.35%

